AFRL-AFOSR-JP-TR-2024-0051

Viscoelastic Characterization and Modeling of the pH-Responsive MXene/Chitosan Composite Foams for Wearable Devices

IL YUB CHOI
SUNGKYUNKWAN UNIVERSITY RESEARCH & BUSINESS FOUNDATION
2066,SEOBU-RO, JANGAN-GU
SUWON-SI, ,
KOR

02/15/2024
Final Technical Report

Air Force Research Laboratory
Air Force Office of Scientific Research
Asian Office of Aerospace Research and Development
Unit 45002, APO AP 96338-5002

REPORT DOCUMENTATION PAGE

PLEASE DO NOT RETURN YOUR FORM TO THE ABOVE ORGANIZATION.

1. REPORT DATE	2. REPORT TYPE	3. DATES COVERED	
20240215	Final	START DATE 20220930	END DATE 20230929

4. TITLE AND SUBTITLE
Viscoelastic Characterization and Modeling of the pH-Responsive MXene/Chitosan Composite Foams for Wearable Devices

5a. CONTRACT NUMBER	5b. GRANT NUMBER	5c. PROGRAM ELEMENT NUMBER
	FA2386-22-1-4069	
5d. PROJECT NUMBER	**5e. TASK NUMBER**	**5f. WORK UNIT NUMBER**

6. AUTHOR(S)
Il Yub Choi

7. PERFORMING ORGANIZATION NAME(S) AND ADDRESS(ES)
SUNGKYUNKWAN UNIVERSITY RESEARCH & BUSINESS FOUNDATION
2066,SEOBU-RO, JANGAN-GU
SUWON-SI
KOR

8. PERFORMING ORGANIZATION REPORT NUMBER

9. SPONSORING/MONITORING AGENCY NAME(S) AND ADDRESS(ES)	10. SPONSOR/MONITOR'S ACRONYM(S)	11. SPONSOR/MONITOR'S REPORT NUMBER(S)
AOARD UNIT 45002 APO AP 96338-5002	AFRL/AFOSR IOA	AFRL-AFOSR-JP-TR-2024-0051

12. DISTRIBUTION/AVAILABILITY STATEMENT
A Distribution Unlimited: PB Public Release

13. SUPPLEMENTARY NOTES

14. ABSTRACT
The ability of intelligent polymer foams to change their structure and volume phase in response to external stimuli such as temperature, pressure, light, pH, solvents, electrical, and magnetic files has opened up new opportunities for advanced technologies. It is also important due to its potential in soft robotics and wearable electronics. In order to optimize the responses to external stimuli and have outstanding mechanical properties, geometric design plays a critical role. However, the parameters of conventional manufacturing techniques restrict the structural geometric design, and the poor mechanical properties of the foams limit their applications. Therefore, by providing synergistic effects of internal structures and intrinsic material properties, hierarchically porous structured foams will be successfully fabricated because distinct three-dimensional (3D) structures can demonstrate optimized properties of low density, the ability to recover from large deformation, and high mechanical properties. Additionally, sufficient characteristics can be provided to materials in areas requiring different functions by controlling their internal structure. Thus, in this proposal, we propose highly viscoelastic, compressible, and pH-responsive wearable devices (e.g., wearable strain sensor for real-time sweat volume monitoring) by incorporating synergistic effects of Ti3C2Tx MXene, an emerging two-dimensional (2D) nanomaterial, and chitosan, a natural polymer.
Moreover, we will systematically investigate viscoelastic properties and modeling for pHresponsive MXene/chitosan composite foams to examine further characterization. Accordingly, benefiting from the high viscoelastic properties and pH-responsive performance of the foams, they suggest having great potential for wearable electronics, sensing devices, and biomedical applications.

15. SUBJECT TERMS

16. SECURITY CLASSIFICATION OF:			17. LIMITATION OF ABSTRACT	18. NUMBER OF PAGES
a. REPORT U	b. ABSTRACT U	c. THIS PAGE U	SAR	21

19a. NAME OF RESPONSIBLE PERSON	19b. PHONE NUMBER *(Include area code)*
TODD RUSHING	315-227-7003

Standard Form 298 (Rev.5/2020)
Prescribed by ANSI Std. Z39.18

TABLE OF CONTENTS

Page

LIST OF FIGURES

Page

1.0 SUMMARY

In this project, we propose highly viscoelastic, compressible, and pH-responsive wearable devices (e.g., wearable strain sensor for real-time sweat volume monitoring) by incorporating synergistic effects of $Ti_3C_2T_x$ MXene, an emerging two-dimensional (2D) nanomaterial, and chitosan (CS), a natural polymer. Moreover, we will systematically investigate viscoelastic properties and modeling for pH-responsive MXene/chitosan composite foams to examine further characterization. Due to the funding conditions of the support organization, we performed only the first year's work as the following scheme.

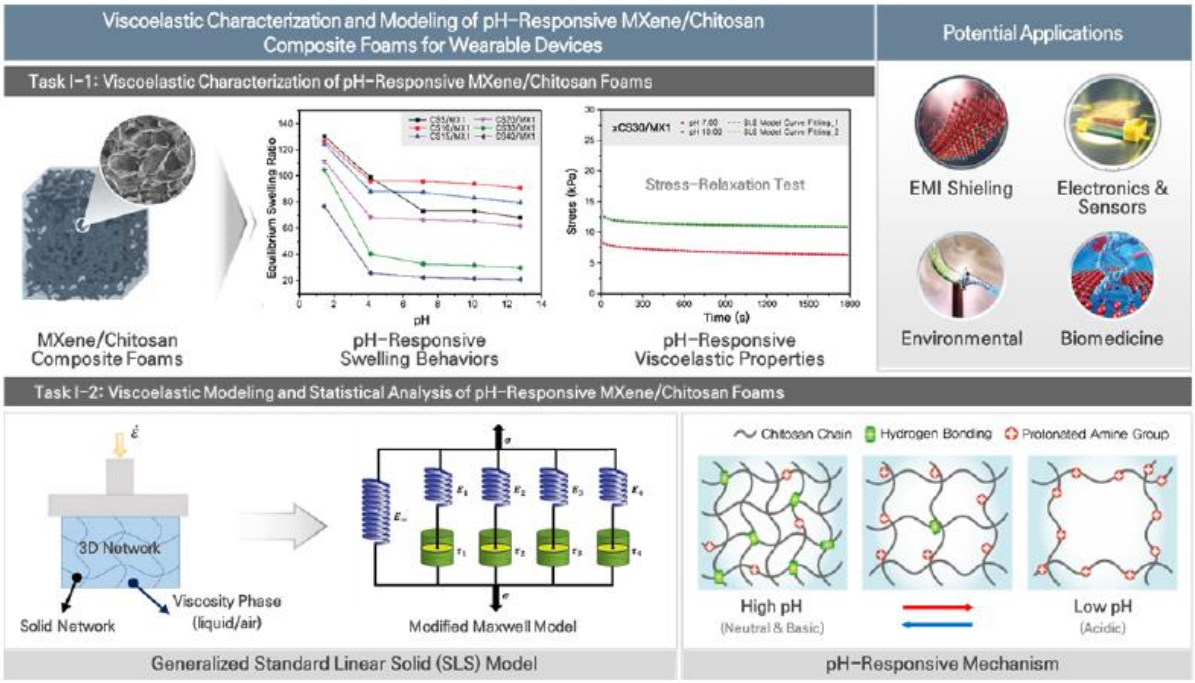

Scheme 1. A schematic illustration of the overall vision of the proposed research.

2.0 INTRODUCTION

The ability of intelligent polymer foams to change their structure and volume phase in response to external stimuli such as temperature, pressure, light, pH, solvents, and electrical and magnetic fields has opened up new opportunities for sophisticated technologies and extensive research [1]. In order to optimize the responses to external stimuli, geometric design plays a vital role. However, the parameters of conventional manufacturing techniques typically restrict structural geometric design. As a result of the synergistic effects of internal structures and material incorporations, hierarchically porous structured foams will be successfully fabricated in this study because the distinct three-dimensional (3D) structure can demonstrate optimized properties of low density, the ability to recover from large deformation, and high mechanical properties. Additionally, sufficient characteristics can be provided to materials in areas

requiring different functions by controlling their internal structure. Therefore, hierarchically structured foams were created to optimize stimuli-response capabilities by incorporating chitosan and MXene.

Chitosan (CS) is a natural linear polysaccharide consisting of *N*–acetyl–*D*–glucosamine and glucosamine units linked with *β*–(1–4) bonds produced from chitin deacetylation, which can be extracted from exoskeletons of crustaceans such as crabs, shrimps, lobsters, and others [2]. Since there are over 10 gigatons of chitin in the biosphere at any given time, CS is one of the most valuable green and renewable resources. It has a large number of hydrophilic groups, including amino and hydroxyl groups, which provide desirable properties and qualities such as biodegradability, biocompatibility, and non-toxicity. Furthermore, using the interaction between the amino groups of CS, self-crosslinking between polymer chains can be provided, resulting in porous architectures. Owning these benefits, intensive research into CS-based materials for various environmental and biomedical engineering applications has been reported [3].

MXene is a recently emerged multifaceted two-dimensional (2D) material that has attracted rapidly growing scientific attention since Gogotsi *et al.* first discovered $Ti_3C_2T_x$ in 2011 due to its exceptional chemical and physical properties providing flexibility and variable composition [4, 5]. MXene is an early transition metal carbide or nitride with the general formula of $M_{n+1}X_nT_x$ ($_n$=1, 2, or 3), where M, X, and T denote the early transition metal, interleaved with *n* layers of carbon or nitrogen, and the surface terminations (−O, −OH, and −F) produced during the synthesis process, respectively [6]. MXene has a conductivity of 6,500 S/cm, which is higher than that of graphene and other solution-processed materials [7]. Moreover, the surface terminations formed during the synthesis process give MXene hydrophilicity and a high surface charge (negative zeta potential exceeding -30 mV) [8], allowing MXene to be easily incorporated with a wide range of materials [9]. Therefore, the desirable combination of superior metallic electrical conductivity and versatile surface functionalities can make MXene suitable for various applications, including energy storage devices, electromagnetic interference shielding, and sensors.

MXene also exhibits strong biological properties with a large surface, good hydrophilicity, and biocompatibility, which appeals to applications in biomedicine and biotechnology [5]. However, keeping their outstanding properties in polymeric composites remains challenging. Therefore, CS, a biocompatible polymer, was used to develop CS/MX foams. Since MXene has hydrophilicity and high surface charges generated during the synthesis process, it allows the incorporation of MXene with CS through covalent bonds, hydrogen bonds, or electrostatic interactions. Therefore, the desirable combination of structure and property with versatile surface functionalities can make MXene suitable for diverse applications.

However, CS/MX foams with one-step crosslinking cannot sustain their structural stability in solvents or any other aqueous environment, so a further crosslinking process is required. Thus, this study prepared xCS/MX foams by a two-step crosslinking reaction followed by freeze-drying methods.

A two-step crosslinking reaction provided a well-defined network structure with solvent stability and novel compressibility by providing strong bonding interactions. Their chemical compositions, structural morphologies, thermal, mechanical, and viscoelastic properties were also characterized in addition to moisture- and solvent-responsive performance from swelling measurement. Inspired by the unique properties and structures of CS and MXene, this study investigates how to replicate them in stimuli-responsive composites, allowing enhanced mechanical properties and exploiting the promising stimuli-responses. Therefore, further research into the developed xCS/MX foams by optimizing the structure-property relationship and stimuli-responsive performance can provide flexible design characteristics for various potential engineering applications.

3.0 METHODS, ASSUMPTIONS, AND PROCEDURES

3.1 Materials

Ti_3AlC_2 (MAX phase; high purity = 99.99%) was purchased from Jilin 11 Technology Co., Ltd. CS powder with medium molecular weight (viscosity = 200 − 800 cps at 25°C with 1% acetic acid, deacetylation degree = 75 − 80%), acetic acid (ACS reagent, ≥ 99.7%), and formaldehyde solution (FA; 37 wt% in H_2O) were purchased from Sigma-Aldrich. Lithium fluoride (LiF; 98.5%) powder was obtained from Alfa Aesar. Hydrochloric acid (HCl, 35 – 37%) and buffer solutions (pH 1.00, 4.00, 7.00, 10.00, and 13.00) were purchased from Daejung Chemical & Materials Co., Ltd. All the reagents were laboratory grade and used without further purification and deionized (DI) water was used as working fluid throughout the experiment.

3.2 Synthesis of $Ti_3C_2T_x$ MXene

$Ti_3C_2T_x$ MXene was synthesized by utilizing the minimally intensive layer delamination (MILD) method to achieve larger flake sizes, which are more resistant to oxidation due to the low density of faults and corners in larger flakes. For the first step, 3 g of LiF was completely dissolved in 12 M HCl at room temperature to obtain the etchant solution. Then, 3 g of Ti_3AlC_2 powder was slowly added to the above etchant solution under vigorous magnetic stirring, followed by a continuous reaction for 24 h at room temperature. Subsequently, the resulting acidic product was washed repeatedly with DI water via centrifugation (3,500 rpm for 20 min) until the pH of the supernatant reached around 6.00. $Ti_3C_2T_x$ sediment was then dispersed in 50 mL of DI water and tip sonicated for 30 min to delaminate the multilayered $Ti_3C_2T_x$ clay. Finally, the few-layered MXene suspension was obtained after centrifugation at 3500 rpm for another 20 min and dried by lyophilization of the supernatant.

3.3 Preparation of xCS/MX Foams

xCS/MX foams were synthesized with CS, MXene, and FA by the solution-based freeze-drying method incorporating a two-step crosslinking reaction (Figure 3-1). CS powder was dissolved in a 1 wt% of aqueous acetic acid solution at six different concentrations (5, 10, 15, 20, 30, and 40 mg/mL) to obtain CS solutions. Then, MXene suspension was prepared with 1 mg/mL concentration in DI water. Subsequently, MXene suspension was added to CS solutions at a 1 : 1 (CS : MX) volume ratio and tip sonicated for 30 min at 10°C to get CS/MX mixtures to initiate the first-step crosslinking reaction between CS and MXene. After obtaining the CS/MX mixtures, FA solution was added to the mixtures and stirred for 10 min to achieve the second-step crosslinking reaction producing crosslinked CS/MX (xCS/MX) mixtures. The molecular weight ratio between FA and CS is 1.25 to provide a complete reaction between CS, MXene, and FA. xCS/MX mixtures were lyophilized at −80°C for 72 h to obtain xCS/MX foams. In addition, MXene foams without crosslinking reactions were also prepared by freeze-drying of MXene suspension at −80°C for 72 h. The dimensions of the samples were measured to be 18 mm in diameter and 13.5 mm in height, having light grey color. Their weights and densities were determined before every characterization.

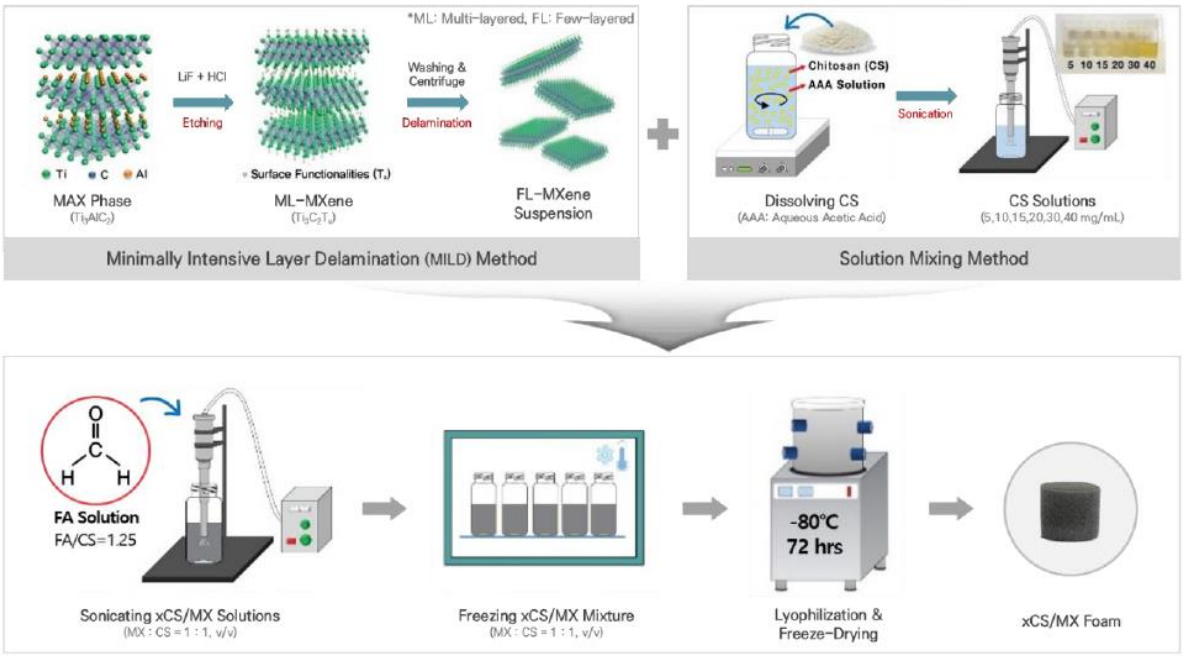

Figure 3-1. Schematic of the synthesis procedure of xCS/MX foams: the preparation of the (a) MXene from minimally intensive layer delamination (MILD) method, (b) CS solutions with varying concentrations (5, 10, 15, 20, 30, and 40 mg/mL), and (c) the preparation and solution-based freeze-drying of xCS/MX mixtures and the resulting xCS/MX foams.

3.4 Material Characterization

Field emission scanning electron microscopy (FE-SEM, JSM-7600F, JEOL) was used to examine the structural morphologies of the foams and to determine elemental compositions. X-ray diffraction (XRD) data were recorded with a SmartLab X-ray diffractometer using Cu-Kα radiation in the 2θ range of 3 to 70° at a scanning speed of 4°/min. Fourier transform infrared (FT-IR) spectroscopy was obtained by an attenuated total reflection infrared spectrometer (IFS-66/S, TENSOR27, Bruker) from 400 to 4,000 cm^{-1} at a relative scan rate of 110 scan/sec. The resolution and wavenumber accuracies are 0.1 and 0.01 cm^{-1}, respectively.

3.5 pH-Responsive Performance

The pH-responsive performance tests of the foams in different pH solutions (pH 1.00, 4.00, 7.00, 10.00, and 13.00) were observed at room temperature. To observe the swelling behaviors, including the equilibrium swelling ratio, the foams were placed in the vials filled with different pH solutions and held at room temperature for 48 h. The weight and dimensions of the foams were measured by immersion of the foams in the solutions at different time intervals (30 s, 1 min, 3 min, 5 min, 10 min, 30 min, 1 h, 12 h, 24 h, and 48 h).

3.6 Mechanical and Viscoelastic Tests

In addition, compression and stress-relaxation tests were performed using the universal testing machine (ElectroPuls E3000, Instron) equipped with a 250 N load cell. The foams were placed between two cylindrical indenters with smooth flat plates. An initial preload of 0.01 N was applied to the foams to ensure complete contact between the loading indenter and the foams. For the cyclic compression test, 30% of strain was applied with 10% strain/min of ramp rate for 1,000 cycles. For the stress-relaxation test, the foams were compressed to 80% of strain, beyond the purely elastic region, at the loading rate of 10% strain/min and held compressed for 30 min. Importantly, all the foams used for the pH-responsive performance tests were cylindrical shapes with approximately 18 mm in diameter and 13.5 mm in height. Also, the foams were dried in a vacuum oven at 50°C for 12 h before immersion in the solutions.

4.0 RESULTS AND DISCUSSION

4.1 Chemical mechanism

The chemical mechanism for the synthesis of xCS/MX foams by different crosslinking reactions is shown in Figure 4-1. The first crosslinking reaction occurred by mixing CS and MXene, which only contains physical crosslinking. Two different interactions are likely to occur at the organic-inorganic interface between the negatively charged surface terminations of the MXene and the positively charged nitrogen-containing amino groups of CS. Firstly, the abundant –OH groups on CS chains would form hydrogen bonds with the surface terminations of MXene, including –OH, –O, and –F, resulting in the intercalation of MXene by CS chains. Secondly, the –OH groups on MXene can react with the –OH groups or protonated amine groups of CS to form non-covalent bonds by electrostatic forces. Non-covalent interactions are critical in maintaining the 3D structure by large molecules. These interactions also heavily influence the crystallinity and design of materials, particularly for self-assembly, and in general, the synthesis of many organic molecules.

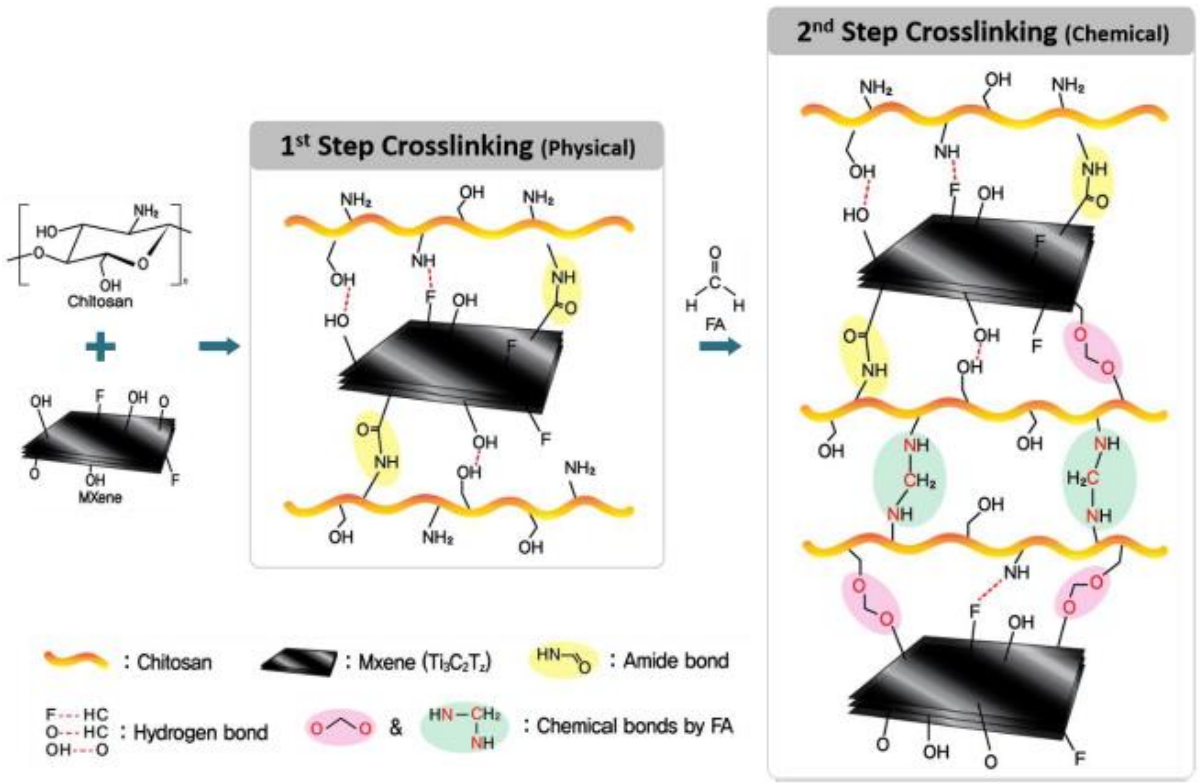

Figure 4-1. The chemical mechanism for fabricating xCS/MX foams by two-step crosslinking reaction.

The second crosslinking was developed by adding an FA solution. The surface functional group made MXene highly dispersive in water and offered reactive sites for chemical crosslinking to prepare a stable structure. Surface terminal groups like –OH and –O of MXene and –OH groups of CS react with FA and form O–C–O linkages, highlighted with pink in Figure 4-1. Then, self-crosslinking was also expected between CS molecules by employing the reaction between amino groups of CS and carbonyl groups of FA. They are highlighted in green in Figure 4-1. Here, the crosslinking between CS and MXene and CS and CS are expected, but the self-crosslinking between MXene molecules is unlikely to form because the content of MXene in the foam is low (between 0 and 10%) and assumed that it is homogeneously distributed in CS polymer matrix.

4.2. Materials characterization

The structural transition from the MAX phase to MXene is confirmed by XRD patterns shown in Figure 4-2a. Compared to the peaks, the (002) peak shifted from 9.5 (MAX phase) to 7.1 (MXene), showing an increase in the interlayer distance caused by the removal of the Al layer and introduction of the surface terminations. The FE-SEM of the MXene is then conducted for additional research (Figure 4-2b). The FE-SEM images of MXene revealed a few-layer structure of the MXene sheet and successful

delamination of the MAX phase. The lateral dimensions of the MXene are measured to be between 1 and 5 μm, and the average height of the MXene is around 1 to 3 nm indicating a multilayer structure. The large lateral size of the MXene can be expected to provide exceptional mechanical properties as well as outstanding electrical conductivity on the MXene incorporated nanocomposites. The FT-IR spectra were conducted to identify functional groups in CS, MXene, and xCS/MX foams (Figure 4-2d). For MXene absorption peaks (shown in pink), the stretching vibrations of the strong hydrogen-bonded O–H group and C–F group in the MXene were ascribed at ~3527 and ~1085 cm^{-1}, respectively. For CS (shown in green), typical CS bands were observed at 3450 (hydroxyl group), 1654 (amide I), and 1578 cm^{-1} (amide II). The presence of amide deformation in the FT-IR spectra of the CS and xCS/MX foams implies successful crosslinking. As shown by the negligible differences between the spectra of the CS and xCS/MX foams, the crosslinking of the CS was unaffected by the addition of MXene sheets. The characteristic peak of xCS/MX foams shows a broad absorption band at ~3638 cm-1, which is attributed to the stretching vibration of strongly hydrogen-bonded O–H groups of MXene and CS. Most notably, two new peaks were observed indicating O–C–O linkage between CS and MXene, and self-crosslinking between CS due to FA.

The controllable microstructures, such as hierarchical open-, semi-open-, and closed-cell structures, are designed and synthesized by varying the CS concentration. The hierarchical porous morphology of xCS/MX foams were examined and identified by the FE-SEM images. The photographs and FE-SEM images were used to depict the morphology of freeze-dried MXene (Figure 4-3a) and xCS/MX foams (Figure 4-3b). The freeze-dried MXene foams are very lightweighted but extremely brittle. It decomposed very quickly into powder due to randomly oriented MXene sheets. For xCS/MX foams, although foams have a cellular structure, the pore size is widely ranged from a few μm to 100 μm. When comparing highly concentrated foams to lower concentrated foams, the internal microstructures of the higher concentrated foams showed more homogeneous pore size distribution, as shown in these images, and even obtained higher density. In contrast to the microstructure of CS/GO foams developed in previous study, xCS/MX foams have more lightly closed-cell structure (even feather-like structures) with thinner cell walls.

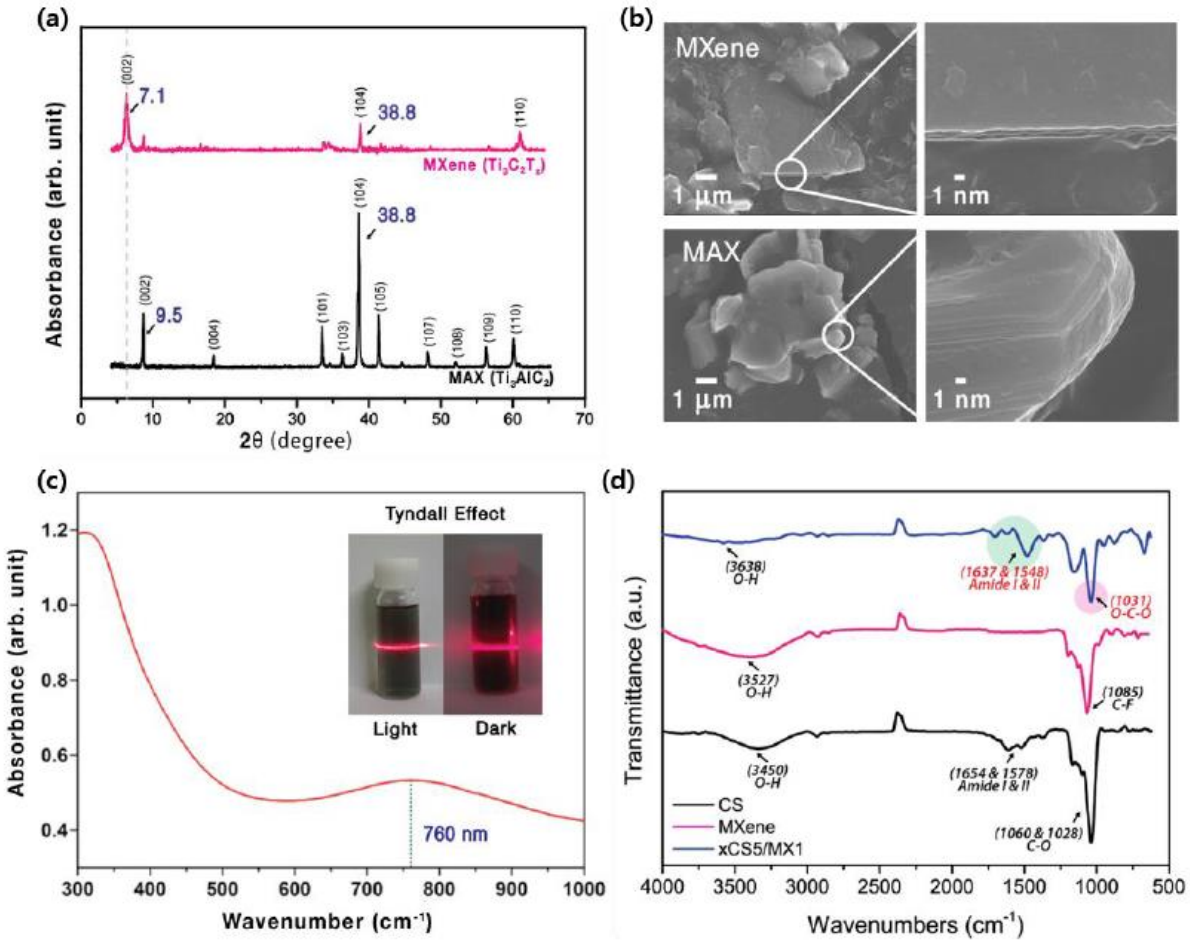

Figure 4-2. Different characterizations for MAX phase, MXene, and xCS/MX foams: (a) XRD spectra, (b) FE-SEM images, (c) UV-vis and Tyndall effect, and (d) FT-IR.

It might be related to the crosslinking density. GO with abundant –COOH and –OH groups are expected to have higher crosslinking density and stronger interfacial bonding strength than MXene with –O, –OH, and –F groups. Consequently, the enhanced crosslinking density could provide CS/GO foams with higher interconnectivity than that of xCS/MX foams. In addition, energy dispersive X-ray spectroscopy (EDS) was taken to check the elemental compositions of xCS/MX foams (Figure 4-4). Element C, O, N, Ti, and F were determined to have 46.30, 43.15, 1.32, 4.29, and 4.94%, respectively.

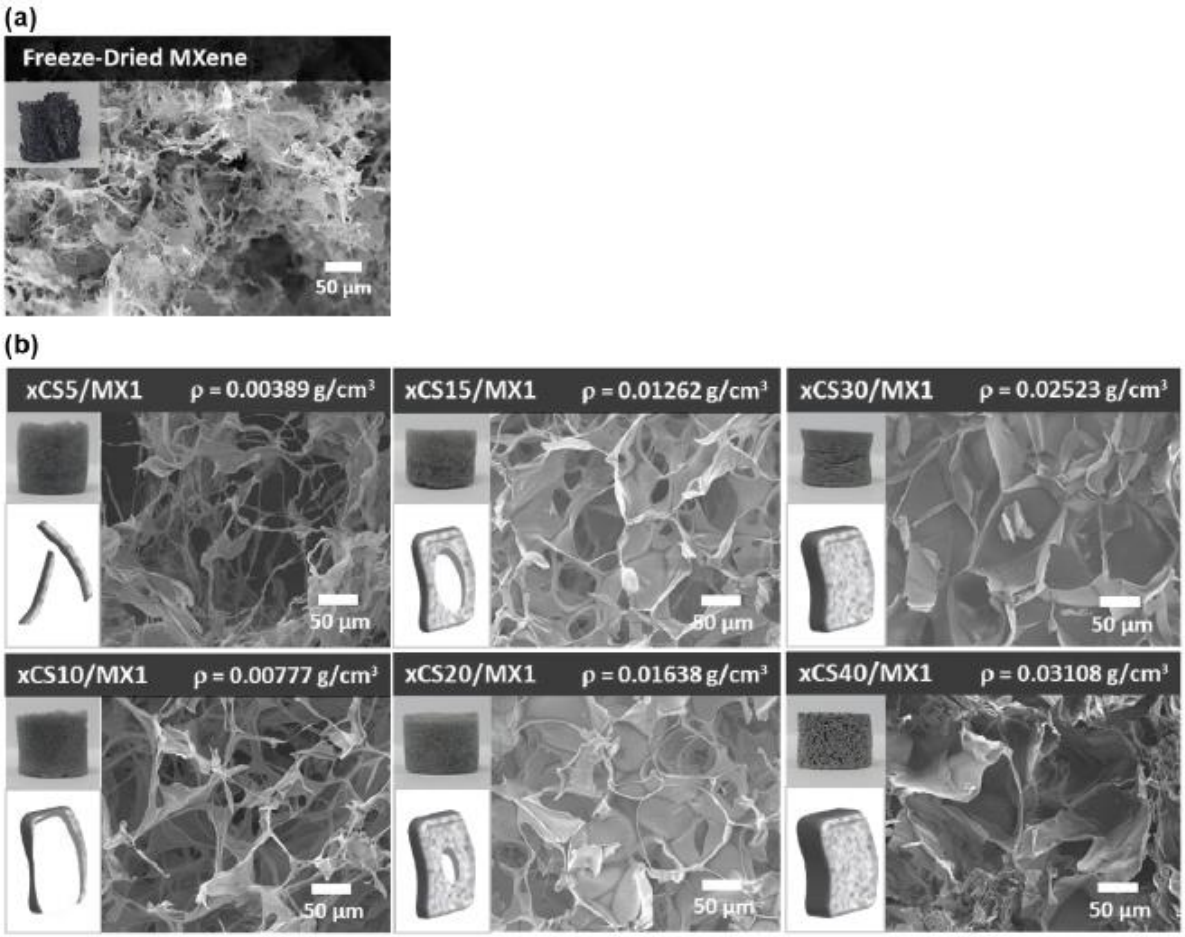

Figure 4-3. FE-SEM images and photographs of (a) freeze-dried MXene foams and (b) xCS/MX foams with different CS concentrations with schematic illustration of cellular structures.

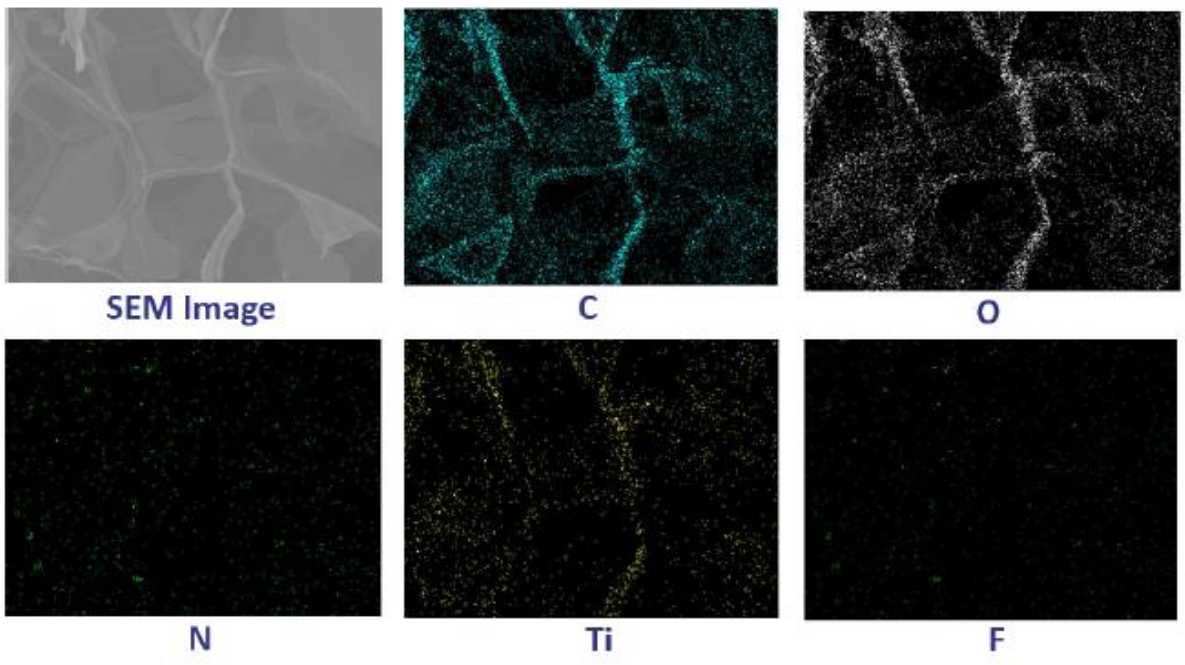

Figure 4-4. EDS of xCS/MX foams, including elements C, O, N, Ti, and F.

4.3 Structural Stability in Water

The swelling test is conducted to confirm the structural stability of the freeze-dried MXene, CS/MX foams, and xCS/MX foams (Figure 4-5). The freeze-dried MXene (i.e., without crosslinking) decomposed very quickly (within 1 min) after being placed in water. The hydrophilic nature of the surface terminations (–F, –O, and –OH groups) made the freeze-dried MXene lacks insufficient structural stability. CS/MX foams prepared by one-step crosslinking reaction began to decompose after 5 min or 1 h, depending on the CS concentration, and were completely decomposed after 12 h. They retained their structure a little longer than the freeze-dried MXene, but they were not strong enough to withstand external forces such as handshaking. This might be due to the hydrogen bonds that exist between the MXene and CS molecules, which can be disrupted by mechanical forces. Therefore, to enhance the structural stability of the foams in water, further crosslinking process is necessary. xCS/MX foams prepared by a two-step crosslinking reaction by adding FA as a crosslinking agent are examined. The foams demonstrated significant swelling behavior in water. They preserved their cylindrical shape after being immersed for 24 h and even longer than several months. Moreover, the foams remained their shape after applying external forces like handshaking and vibration. This behavior is due to the chemical covalent bonds created during the second-step crosslinking reaction that can provide xCS/MX foams with a well-defined network structure and strong bonding interactions between CS, MXene, and FA.

Subsequently, the equilibrium swelling ratio and the CS concentration-dependent behavior of xCS/GO foams are investigated (Figure 4-6). The swelling ratio was calculated using Equation (4-1)

$$Q = \frac{W_S - W_d}{W_d} \times 100\% \tag{4-1}$$

where W_s is the weight of swollen hydrogels and W_d is the weight of dried hydrogels. As shown in Figure 4-6a, all foams expanded rapidly at first 5 min and gradually increased the swelling ratio until 1 h. Finally, foams attained the stable equilibrium swelling after 5 h. Once they reached the equilibrium swelling ratio, they maintained their structure for over several months and resisted external forces. This is because water molecules are attracted to the –OH groups of hydrophilic CS and MXene and permeate into the foam to attain final equilibrium. In terms of CS concentration, a higher swelling ratio is achieved when increasing the CS concentrations.

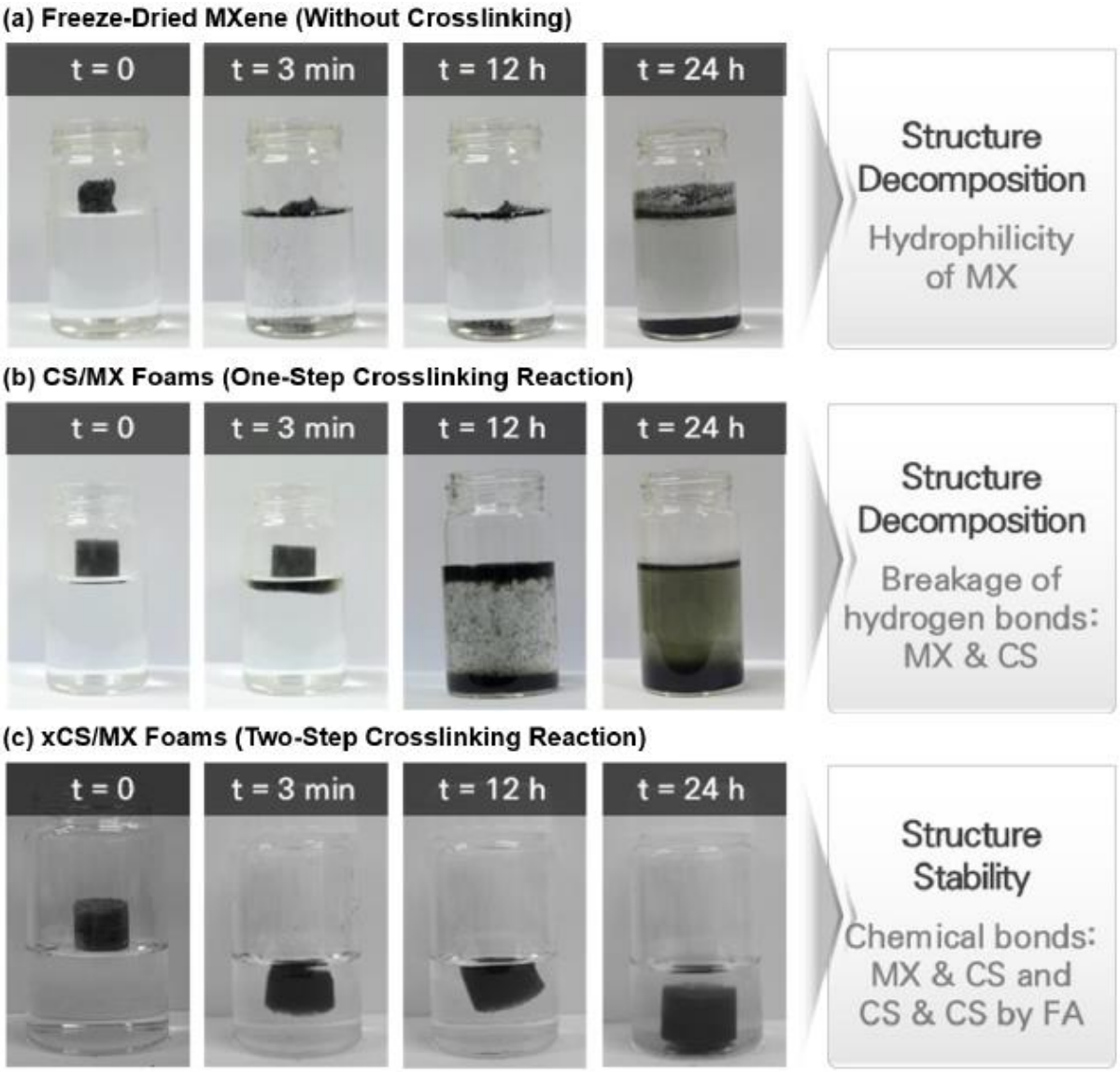

Figure 4-5. Stability in the water of freeze-dried MXene, CS/MXene, and xCS/MXene foams.

This swelling behavior is responsible for not only the hydrogen bonds between water molecules and CS and MXene, but also the chemical covalent and hydrogen bonds between CS, MXene, and FA. Chemical covalent bonds interacted between CS, MXene, and FA during the second-step crosslinking reaction provides the foams with a well-defined network structure and strong bonding interactions. In addition, the hydration effect also helped the foams to swell. Because of the hydration effect, the polymer chains in the foams can catch nearby water molecules through strong interactions such as hydrogen bonding, resulting in bound water. In contrast, the water molecules isolated from the polymer chains, also known as free water, share identified properties with bulk water. As shown in Figure 4-6b, the swelling ratio was decreased by increasing the CS concentration due to crosslinks produced by FA. This behavior is also explained by elastic restraining force. As the network expands, CS chains are compelled to assume more elongation but less likely configuration. As a result, the swelling capacity

decreases as the crosslinking ratio increases. The cumulative results show that the crosslinking swelling ratio and crosslinking ratio are affected by the CS concentration.

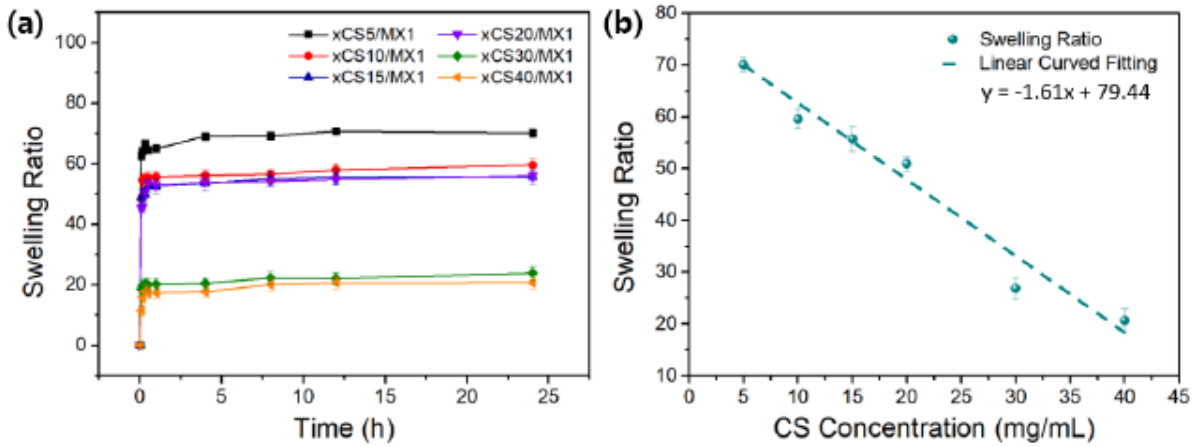

Figure 4-6. (a) Equilibrium swelling ratio and (b) CS concentration-dependent swelling ratio behavior or xCS/MX foams.

4.4 Structural Stability in Various pH Solutions

As seen in Figure 4-7a-b, there is a considerable variation in swelling between pH levels and CS concentrations. In terms of pH, the maximum swelling was observed at low pH of 1.00, and it dramatically decreased between pH 1.00 and pH 4.00, then gradually reduced as the pH of the solution increased for all foams (~pH 13). In terms of CS concentration, the swelling ratio decreases as CS concentration increases. This pH-responsive swelling behavior is based on the protonation and deprotonation of amino groups in CS (Figure 4-7c-d). At low pH, acidic condition, the amide groups ($–NH_2$) on CS can be protonated to form hydrophilic amino groups ($–NH_3^+$). The ensuring electrostatic repulsion between the protonated amino groups weakened the intermolecular and intramolecular hydrogen bonding interaction of CS molecules. As a result, the pH solution can diffuse into the polymer network easily, and eventually reaching equilibrium. On the other hand, at high pH, neutral and basic conditions, no such protonation occurred. Repulsion in the polymer chains recedes resulting in the network shrinkage. Consequently, the swellability of the foams remained relatively low or even unchanged in the basic state. Therefore, it was shown that xCS/MX foams could be successfully used as a biomedical application, specifically as drug delivery carrier that exhibits pH-dependent drug release behavior.

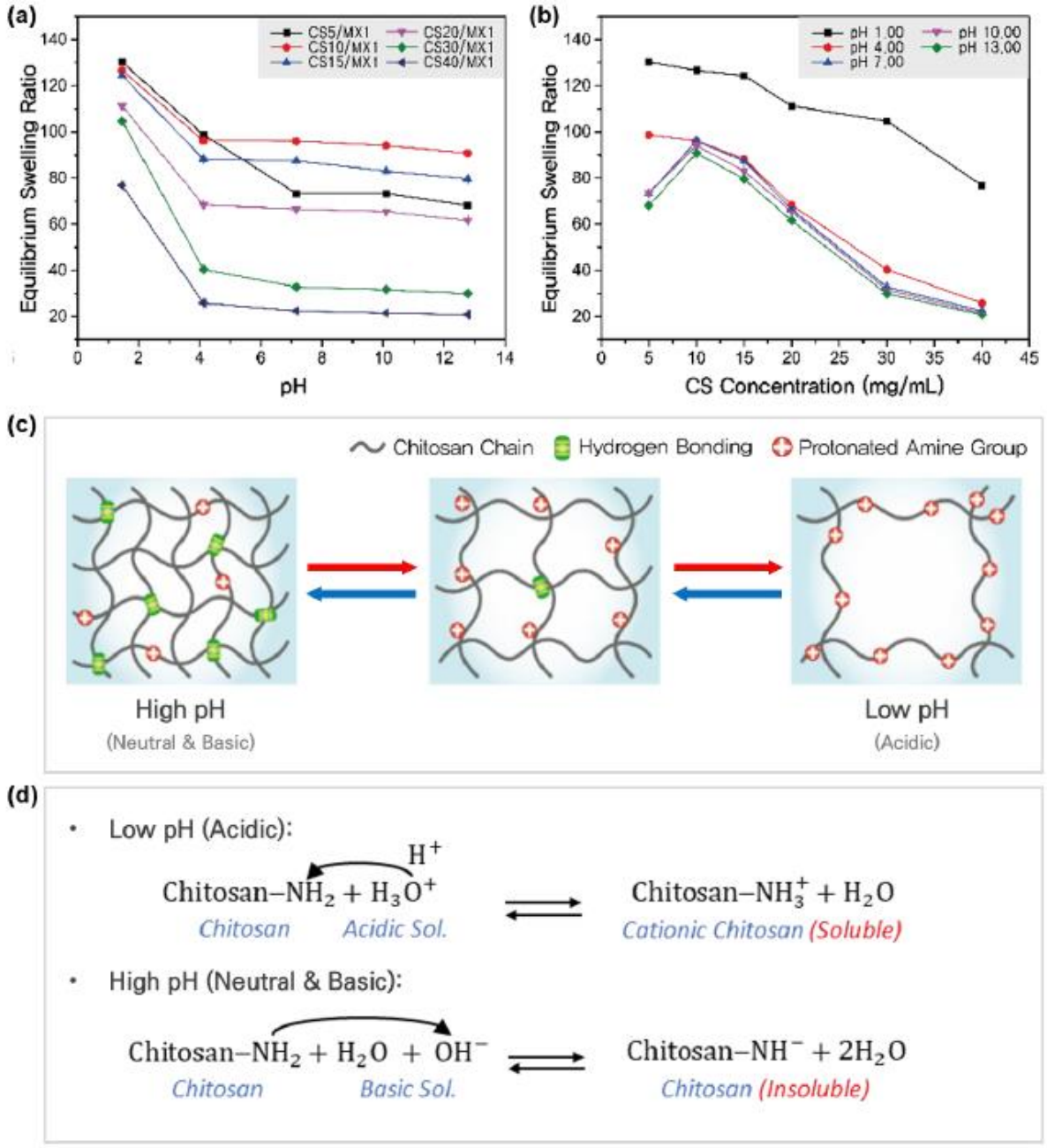

Figure 4-7. Equilibrium swelling ratio of xCS/MX foams with respect to (a) pH levels and (b) CS concentrations. The pH-responsive swelling mechanism is described in (c) schematic and (d) chemical reaction mechanisms.

4.5 Mechanical Characterization

The degree of swelling is a critical parameter that influences the solvent patterns in the polymer network [10]. Furthermore, the swelling rate of different foams varies depending on the pH of the aqueous media [11-13]. Since the purpose of investigating the pH-responsive structure-property relationship is to check the feasibility of the xCS/MX foams used for biomedical applications, the type

of foams and pH levels were selected based on the above characterizations. Here, xCS30/MX1 was selected because it has a closed-cell structure with high compressibility, which gives excellent structural stability and compressibility in water. Furthermore, pH 7.00 and pH 10.00 were chosen for swelling media because most biomedical applications like drug delivery and biosensors are used at the human body system level. Once the specific type of the foams and testing media has been selected, further characterizations. In order to examine the mechanical stability, compressibility, and durability of the xCS30/MX1, the compressive cyclic test was conducted in different media of pH 7.00 and pH 10.00 at 25°C. For the monotonic compression test, the foams were compressed to 80% at 10% strain/min. The compressive strength and Young's moduli were measured at approximately 3.124 and 4.201 kPa at pH 7.00 and 26.23 and 47.93 kPa at pH 10.00, respectively (Figure 4-8a-b). The results demonstrated that xCS30/MX1 exhibited a smart and adaptable response of mechanical flexibility with respect to the pH in which they are immersed. In addition to the monotonic compression test, the compressive cyclic test was performed by applying 50% strain at 0.075 Hz up to 1,000 cycles to observe the compressibility and durability during long-time cyclic loading of the foams. As Figure 4-8c-d shows, both hysteresis loops for pH 7.00 and 10.00 are almost overlapped and remained almost consistent, which leads to no significant difference between dissipation energies during all cycles. This also concludes that the foams are highly reversible and have no permanent bond breakage during compression. Furthermore, it is found that the foams can still endure the compression and come back to the initial geometry and stress-free state even after 1,000 compressive cycles, indicating their outstanding mechanical durability and structural stability. During the cyclic compressions, upon unloading, the flexible molecular segments of CS chains will stretch out spontaneously, and the foams can come back to their original shape. This behavior is significantly related to the protonation and deprotonation of amino groups in CS. When the pH increases, electrostatic repulsion recedes due to deprotonation of amino groups in CS, and strong interaction between hydrogen bonds results in the shrinking of the polymer network. On the other hand, when pH decreases, hydrogen bonding is weakened due to the protonation of the amino group, and the distance between polymer chains is increased, resulting in volume expansion and weakening of the mechanical properties. Therefore, based on the structural stability, compressibility, durability, and pH sensitivity, xCS30/MX1 could be successfully used in a biomedical application, specifically as a drug delivery carrier that exhibits pH-dependent drug release behavior as a composite foam.

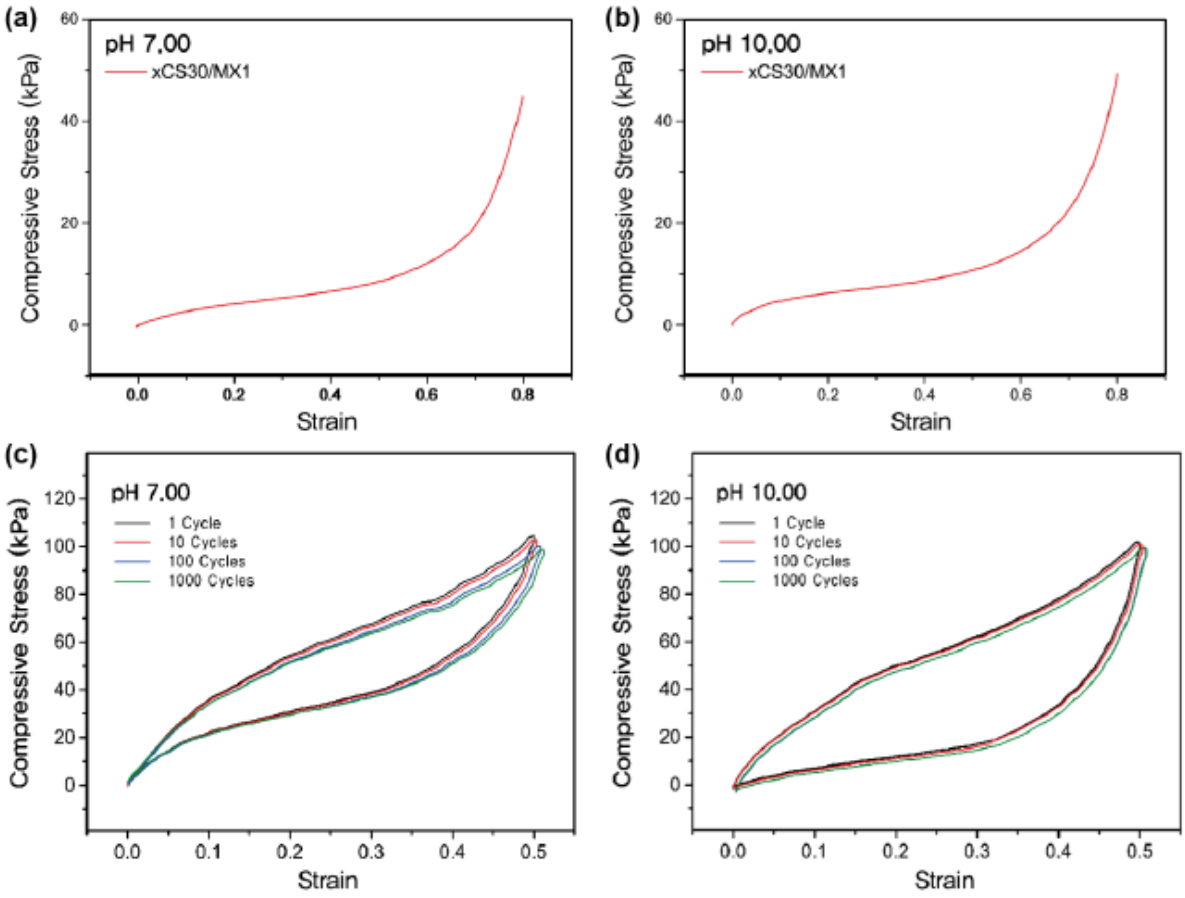

Figure 4-8. Compressive stress-strain curves for (a) monotonic compression test (80% strain, 10% strain/min), and (b) cyclic test (50% strain, 0.075 Hz, 1,000 cycles).

4.6 Stress-Relaxation Characterization

For the stress-relaxation test, the foams were compressed to 80% strain, beyond the purely elastic region, at the loading rate of 10% strain/min and held compressed for 30 min (Figure 4-9). The typical stress-relaxation response of the foams was prepared with different pH values and CS concentrations. The stress gradually decreases over time and finally reaches the equilibrium state, which reflects the static viscoelastic properties (Figure 4-9a). The equilibrium modulus, viscous, and relaxation time were determined by characterizing the stress-relaxation curves obtained using a generalized SLS model. Here, the Maxwell model was used with a linear combination of the elastic and viscous components represented by springs and dashpots. The modified Maxwell model with five springs and four dashpots in series was employed as follow:

$$\sigma(t) = E_\infty + E_1 e^{-\frac{t}{\tau_1}} + E_2 e^{-\frac{t}{\tau_2}} + E_3 e^{-\frac{t}{\tau_3}} + E_4 e^{-\frac{t}{\tau_4}} \quad (4\text{-}2)$$

where E_∞ is the equilibrium modulus representing the elastic modulus of the long-term spring element; E_1, E_2, E_3, and E_4 are the viscous moduli representing the elastic moduli of the springs; and τ_1, τ_2, τ_3,

and τ_4 are the relaxation times of the dashpots. The model takes into consideration that relaxation occurs at a set of time moments and not in a single time moment. It is clearly observed that this modified Maxwell model fits the experimental data well.

For the equilibrium modulus, a higher equilibrium modulus was observed at pH 10.00 because the polymer network becomes more solid as the interaction between hydrogen bonds increases. Due to the deprotonation of amino groups in CS, a much stronger interaction between hydrogen bonds occurred to provide shrinkage of polymer network at pH 10.00 than pH 7.00 (Figure 4-9b). For the viscous modulus, a lower viscous modulus was achieved at pH 10.00. Viscous modulus is related to the friction forces between the polymer network and aqueous media against the applied compressive force. Since the volume of the swollen foam decreased due to deprotonation, there is less possibility to make friction between the polymer network and pH solutions (Figure 4-9c). Lastly, for the relaxation time, a longer relaxation time was required at pH 10.00 because the time to stabilize the polymer chains and molecular mobility during newly forming hydrogen bonding takes longer (Figure 4-9d). In addition to the numerical results, "*" indicates a significant difference between objects of comparison as P-value in the student T-test is less than the critical value, which is 0.05.

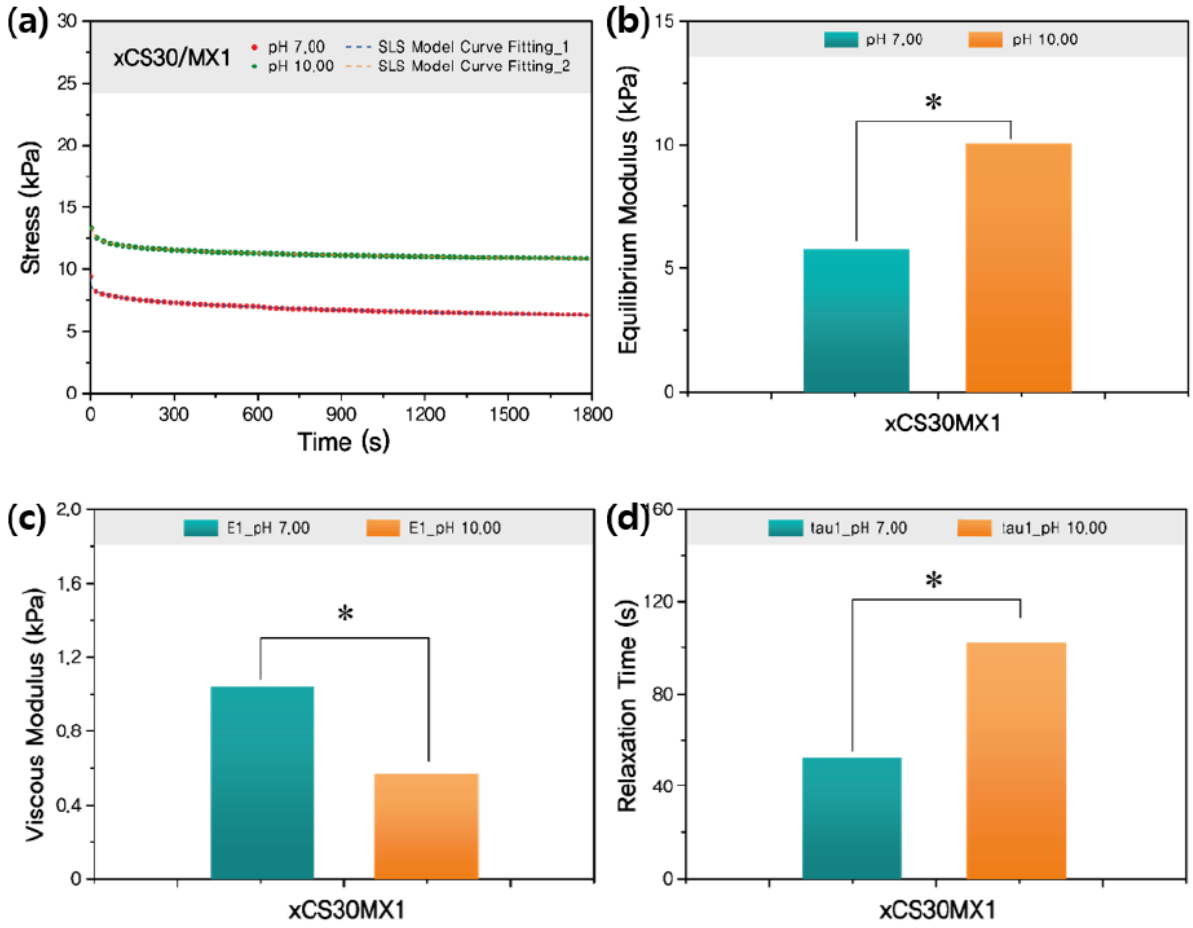

Figure 4-9. Static viscoelastic properties of xCS/MX foams: (a) Stress-relaxation behavior of the xCS/MX foams under a constant strain deformation of 30%. The stress-relaxation response was fitted with the generalized Maxwell model using Equation (4-1). (b) Equilibrium and (c) viscous moduli of the xCS/MX foams are determined by fitting curves drawn using the generalized Maxwell model. (d) The relaxation time of the xCS/MX foams is obtained for the time at which the stress relaxes to 1/e of its initial value.

5.0 CONCLUSIONS

Stimuli-responsive materials can display remarkable changes in their chemical or physical properties upon exposure to external stimuli. As a result, they have raised significant attention for a diverse range of applications. CS is a biodegradable natural polymer having biocompatibility and flexibility but is limited by low mechanical properties. Some researchers have investigated nano-reinforced composites to overcome this challenge, but they may cause a high loading fraction, viscosity problem, and inhomogeneous dispersion. Therefore, since MXene has a high surface area and excellent mechanical and hydrophilic properties, this study used MXene to allow the incorporation of CS to develop the desirable combination of structure and properties. Furthermore, since CS/MX foams with one-step crosslinking cannot sustain their structural stability in aqueous environment, a further crosslinking process is employed to have xCS/MX foams. Therefore, this study investigated hierarchically structured xCS/MXene foams by optimizing the structure-property relationship and stimuli-responsive performance to provide flexible design characteristics.

In conclusion, xCS/MXene foams were successfully developed by a solution-based freeze-drying method using a two-step crosslinking mechanism, and the various properties of the foams were systematically investigated. The foams improved flexibility and swellability in different aqueous media. They also provided pH-responsive properties for practical biomedical applications. The compressive mechanical results showed that an increase in the CS concentration in the foam could significantly enhance the flexibility and swelling property of the foams. Different characterizations also confirmed the homogeneous and porous network of the foams, probably due to the interactions between CS and MXene in the foams. Moreover, xCS30/MX1 were significantly dependent on the pH of the medium. Furthermore, xCS30/MX1 were suggested to have great potential for biomedical applications.

6.0 REFERENCES

1. M. A. C. Stuart et al., Emerging applications of stimuli-responsive polymer materials. Nature materials 9, 101-113 (2010).
2. S. Islam, M. Bhuiyan, M. Islam, Chitin and chitosan: structure, properties and applications in biomedical engineering. Journal of Polymers and the Environment 25, 854-866 (2017).

3. S. Saravanan, R. Leena, N. Selvamurugan, Chitosan based biocomposite scaffolds for bone tissue engineering. International journal of biological macromolecules 93, 1354-1365 (2016).
4. M. Naguib et al., Two-dimensional nanocrystals produced by exfoliation of Ti3AlC2. Advanced materials 23, 4248-4253 (2011).
5. A. Zamhuri, G. P. Lim, N. L. Ma, K. S. Tee, C. F. Soon, MXene in the lens of biomedical engineering: Synthesis, applications and future outlook. Biomedical engineering online 20, 1-24 (2021).
6. K. Hantanasirisakul, Y. Gogotsi, Electronic and optical properties of 2D transition metal carbides and nitrides (MXenes). Advanced Materials 30, 1804779 (2018).
7. B. Anasori, M. R. Lukatskaya, Y. Gogotsi, 2D metal carbides and nitrides (MXenes) for energy storage. Nature Reviews Materials 2, 1-17 (2017).
8. H. An et al., Surface-agnostic highly stretchable and bendable conductive MXene multilayers. Science advances 4, eaaq0118 (2018).
9. J. Liu et al., Hydrophobic, flexible, and lightweight MXene foams for high-performance electromagnetic-interference shielding. Advanced Materials 29, 1702367 (2017).
10. A. Zamhuri, G. P. Lim, N. L. Ma, K. S. Tee, C. F. Soon, MXene in the lens of biomedical engineering: Synthesis, applications and future outlook. Biomedical engineering online 20, 1-24 (2021).
11. K. Hantanasirisakul, Y. Gogotsi, Electronic and optical properties of 2D transition metal carbides and nitrides (MXenes). Advanced Materials 30, 1804779 (2018).
12. F. Ganji, F. S. Vasheghani, F. E. VASHEGHANI, Theoretical description of hydrogel swelling: a review. (2010).
13. I. A. Khalil et al., Ciprofloxacin-loaded bioadhesive hydrogels for ocular applications. Biomaterials science 8, 5196-5209 (2020).